Proceedings of the SEM Annual Conference
June 7-10, 2010 Indianapolis, Indiana USA
©2010 Society for Experimental Mechanics Inc.

Nonlocal Microdamage Constitutive Model for High Energy Impacts

Rashid K. Abu Al-Rub[1] and Anthony N. Palazotto[2]

[1]Zachry Department of Civil Engineering, Texas A&M University, College Station, TX 77843, USA, E-mail: rabualrub@civil.tamu.edu
[2]Department of Aeronautics and Astronautics, Air Force Institute of Technology, WPAFB, OH 45433-7765, USA

ABSTRACT
During highly dynamic and ballistic loading processes, large inelastic deformation associated with high strain rates leads, for a broad class of heterogeneous materials, to degradation and failure by localized damage and fracture. However, as soon as material failure dominates a deformation process, the material increasingly displays strain softening and the finite element predictions of ballistic response are considerably affected by the mesh size. This gives rise to non-physical description of the ballistic behavior and mesh-dependent ballistic limit velocities that may mislead the design of ballistic-resistant materials. This study is concerned with the development and numerical implementation of a novel coupled thermo-hypoelasto-viscoplastic and thermo-viscodamage constitutive model within the laws of thermodynamics in which an intrinsic material length scale parameter is incorporated through the nonlocal gradient-dependent damage approach. It is shown through simulating plugging failure in ballistic penetration of high-strength steel targets by blunt projectiles that the length scale parameter plays the role of a localization limiter allowing one to obtain meaningful values for the ballistic limit velocity independent of the finite element mesh density. Therefore, the proposed nonlocal damage model leads to an improvement in the modeling and numerical simulation of high velocity impact related problems.

INTRODUCTION
In light of the increasing requirements for lightweight vehicular and personal protection systems in many industries (e.g. military, defense, and space), low-density advanced composite materials are highly desirable. Examples of those materials are metallic alloys, ceramics, and polymers with heterogeneous microstructures reinforced with hard, stiff, and/or soft particles (inclusions) at decreasing microstructural length scales that range in size from few nanometers (e.g. carbon nanotubes) to few microns (e.g. ceramic or metallic oxide particles). The focus of this study is on the use of those materials to increase the ballistic performance of structural systems under high impact damage loading conditions. Therefore, it is imperative to develop very effective constitutive and computational models that can be used in guiding the design processes of those advanced materials under ballistic loading conditions. The development of such models is also motivated by the large time and money cost of conducting ballistic experiments on such advanced materials such that physically-based and effective theoretical and computational models, as an adjunct to experimental work, can save a lot of this cost and also provide important insights about their ballistic behaviors that are not accessible by experimental routs. Moreover, the accuracy and computational effectiveness of these models are crucial for designing better materials. Therefore, the focus of this paper is on the development of these modeling techniques that specifically address one main important issue: the finite element mesh-dependent ballistic limit velocity predictions. Mesh sensitivity is one of the most critical problems of numerical codes, especially for the analysis of damage localization and failure. As the perforation analysis of a steel plate by a projectile is the most typical impact problem, it is very important to understand the variation of fracture mechanism of projectiles and target plates according to the change of mesh density. This issue cannot be addressed sufficiently when using the classical (local) plasticity or viscoplasticity (rate-dependent plasticity) and damage or viscodamage (rate-dependent damage) theories due to the absence of explicit intrinsic material length scale measures in their constitutive equations. Recently, Abu Al-Rub and co-authors [1-4] successfully used the nonlocal damage theory to solve the mesh-sensitivity problem. Explicit (via the nonlocal gradient-dependent theory) and implicit (via the viscosity) intrinsic length scales of material are introduced as a remedy of the mesh sensitivity problem where those length scales act as localization

T. Proulx (ed.), *Time Dependent Constitutive Behavior and Fracture/Failure Processes, Volume 3*, Conference Proceedings of the Society for Experimental Mechanics Series 15, DOI 10.1007/978-1-4419-9794-4_11, © The Society for Experimental Mechanics, Inc. 2011

limiters. This framework is also used here to solve the high energy impact of steel targets by blunt deformable projectiles. The enhanced nonlocal gradient-dependent theory formulates a constitutive framework on the continuum level that is used to bridge the gap between the micromechanical theories and the classical (local) continuum theories. They are successful in explaining the size effects encountered at the micron scale and in preserving the well-posedeness of the initial boundary value problem governing the solution of material instability triggering strain localization. Moreover, viscosity (rate dependency) allows the spatial difference operator in the governing equations to retain its hyperbolicity and the initial boundary value problem is well-posed. Model capabilities are preliminarily illustrated for the dynamic localization of inelastic flow in adiabatic shear bands and the perforation of Weldox 460E steel plates with by a deformable blunt projectile at various high impact speeds.

NONLOCAL MICRODAMAGE CONSTITUTIVE MODEL

The micro-damage model used to predict material behavior under dynamic loading conditions was earlier presented in [1]. Thus, only the main equations will be given in the following. The model is based on the nonlocal gradient-dependent theory. It includes the von Mises yield criterion, the non-associated flow rules, isotropic and anisotropic strain hardening, strain rate hardening, softening due to adiabatic heating and anisotropic damage evolution, and finally a path dependent equation of state. The stress-strain rate relationship in the spatial and damaged configuration is given by

$$\overset{\nabla}{\boldsymbol{\tau}} = \mathbb{C} : \left(\boldsymbol{d} - \boldsymbol{d}^{vp} - \boldsymbol{d}^{vd} \right) - \boldsymbol{A} : \overset{\nabla}{\boldsymbol{\phi}} - \boldsymbol{\beta} \dot{T}, \quad \mathbb{C} = \widehat{\boldsymbol{M}}^{-1} : \overline{\mathbb{C}} : \widehat{\boldsymbol{M}}^{-1}, \quad \widehat{\boldsymbol{M}} = 2\left[\left(\mathbf{1} - \widehat{\boldsymbol{\phi}} \right) \otimes \mathbf{1} + \mathbf{1} \otimes \left(\mathbf{1} - \widehat{\boldsymbol{\phi}} \right) \right]^{-1} \tag{1}$$

where $\overset{\nabla}{}$ indicates co-rotational objective derivative, $\boldsymbol{\tau}$ is the corotational rate of Kirchhoff stress tensor, $\boldsymbol{d}$ is the total rate of deformation, $\overline{\mathbb{C}}$ and $\mathbb{C}$ are the forth-order undamaged and damaged elasticity tensors, respectively, $\dot{T}$ is the rate of absolute temperature, $\boldsymbol{\beta}$ is the damaged thermal expansion coefficient, and $\mathbf{1}$ is the second-order identity tensor. $\overline{\mathbb{C}}$ and $\boldsymbol{A}$ are given by the following relations:

$$\overline{\mathbb{C}} = K^e \mathbf{1} \otimes \mathbf{1} + 2G^e \mathbf{I}^{dev}, \quad \boldsymbol{A} = \frac{\partial \widehat{\boldsymbol{M}}^{-1}}{\partial \widehat{\boldsymbol{\phi}}} : \widehat{\boldsymbol{M}} : \boldsymbol{\tau} + \mathbb{C} : \widehat{\boldsymbol{M}} : \frac{\partial \widehat{\boldsymbol{M}}^{-1}}{\partial \widehat{\boldsymbol{\phi}}} : \mathbb{C}^{-1} : \left(\boldsymbol{\tau} + \boldsymbol{\beta} \Delta T \right) \tag{2}$$

where K^e is the bulk modulus and G^e is the shear modulus. The viscoplastic rate of deformation, $\boldsymbol{d}^{vp}$, the viscodamage rate of deformation, $\boldsymbol{d}^{vd}$, and the nonlocal second-order damage tensor, $\widehat{\boldsymbol{\phi}}$, are give as follows:

$$\boldsymbol{d}^{vp} = \dot{\lambda}^{vp} \frac{\partial f}{\partial \boldsymbol{\tau}}, \; \boldsymbol{d}^{vd} = \dot{\lambda}^{vd} \frac{\partial g}{\partial \boldsymbol{\tau}}, \; \overset{\nabla}{\boldsymbol{\phi}} = \dot{\lambda}^{vp} \frac{\partial f}{\partial \boldsymbol{Y}} + \dot{\lambda}^{vd} \frac{\partial g}{\partial \boldsymbol{Y}} \tag{3}$$

The potentials f and g are the nonlocal viscoplastic and viscodamage conditions given, respectively, by

$$f = \sqrt{\tfrac{3}{2}\left(\overline{\boldsymbol{\tau}}' - \overline{\widehat{\boldsymbol{X}}} \right) : \left(\overline{\boldsymbol{\tau}}' - \overline{\widehat{\boldsymbol{X}}} \right)} - \left[\overline{Y}_{yp} + \overline{\widehat{R}} \right] \left[1 + (\eta^{vp} \dot{\overline{p}})^{1/m_1} \right] \left[1 - \left(T/T_m \right)^n \right] \le 0 \tag{4}$$

$$g = \sqrt{\left(\widehat{\boldsymbol{Y}} - \widehat{\boldsymbol{H}} \right) : \left(\widehat{\boldsymbol{Y}} - \widehat{\boldsymbol{H}} \right)} - \left[l + \widehat{K} \right] \left[1 + (\eta^{vd} \dot{\widehat{r}})^{1/m_2} \right] \left[1 - \left(T/T_m \right)^n \right] \le 0 \tag{5}$$

where $\overline{\boldsymbol{\tau}}'$ is the effective deviatoric stress tensor, $\overline{Y}_{yp}$ is the initial yield strength (at zero absolute temperature, zero plastic strain, and static strain rate), T_m is the melting temperature, $\overline{\widehat{R}}$ is the nonlocal isotropic hardening stress, $\overline{\widehat{\boldsymbol{X}}}$ is the nonlocal anisotropic hardening stress, $\dot{\overline{p}} = \sqrt{\frac{2}{3} \overline{d}_{ij}^{vp} \overline{d}_{ij}^{vp}}$ is the rate of the effective accumulative viscoplastic strain, m and n are material constants, η^v is the relaxation time, the non-local damage forces $\widehat{\boldsymbol{Y}}$

and $\widehat{K}$ are, respectively, characterizing the viscodamage evolution and the viscodamage isotropic hardening forces, l is the initial damage threshold, and $\widehat{r}$ is the nonlocal damage accumulation.

The nonlocal evolution equation for the isotropic and kinematic hardening in the undamaged configuration, are given as:

$$\dot{\overline{R}} = \dot{\overline{R}} + \tfrac{1}{2}\ell_1^2\nabla^2\dot{\overline{R}} \quad \text{with} \quad \dot{\overline{R}} = \frac{a_1\dot{\lambda}^{vp}}{\left(1-\widehat{r}\right)^2}\left(1-k_1\overline{\widehat{R}}\right) \tag{6}$$

$$\overset{\nabla}{\overline{\boldsymbol{X}}} = \overset{\nabla}{\boldsymbol{X}} + \tfrac{1}{2}\ell_2^2\nabla^2\overset{\nabla}{\boldsymbol{X}} \quad \text{with} \quad \overset{\nabla}{\overline{X}}_{ij} = a_2\dot{\lambda}^{vp}\widehat{\boldsymbol{M}} : \widehat{\boldsymbol{M}} : \left(\frac{\partial f}{\partial \overline{\boldsymbol{\tau}}} - k_2\overline{\widehat{\boldsymbol{X}}}\right) \tag{7}$$

The evolution equations for the nonlocal viscodamage isotropic and kinematic hardening functions are given by

$$\dot{\overline{K}} = \dot{K} + \tfrac{1}{2}\ell_3^2\nabla^2\dot{K} \quad \text{with} \quad \dot{K} = a_3\dot{\lambda}^{vd}\left(1-h_1\widehat{K}\right) \tag{8}$$

$$\overset{\nabla}{\overline{\boldsymbol{H}}} = \overset{\nabla}{\boldsymbol{H}} + \tfrac{1}{2}\ell_4^2\nabla^2\overset{\nabla}{\boldsymbol{H}} \quad \text{with} \quad \overset{\nabla}{\boldsymbol{H}} = a_4\dot{\lambda}^{vd}\left(\frac{\partial g}{\partial \boldsymbol{Y}} - h_2\widehat{\boldsymbol{H}}\right) \tag{9}$$

The nonlocal strain energy release rate is given by

$$\widehat{\boldsymbol{Y}} = \frac{\left(1+a_5\right)}{2}\left(\boldsymbol{\tau}-\boldsymbol{\beta}\Delta T\right) : \widehat{\boldsymbol{M}} : \frac{\partial\widehat{\boldsymbol{M}}^{-1}}{\partial\widehat{\boldsymbol{\phi}}} : \mathbb{C}^{-1} : \left(\boldsymbol{\tau}+\boldsymbol{\beta}\Delta T\right) \tag{10}$$

where ℓ_i (i=1-4) are material length scale parameters which should be obtained from gradient-dominant experiments (e.g. indentation tests, bending tests, or torsion tests) [5]. k_i, h_i, and a_i are material constants that can be identified from conventional tests (e.g. uniaxial tension test). In this study, the material length scales ℓ_i (i=1-4) are assumed equal and physically interpreted as the average free-path for dislocations, such that the following expression has been derived in [6] based on dislocation mechanics arguments:

$$\dot{\ell} = \ell\,\nu_o\exp\left[-\left(U_o/k_BT\right)\left\{1-\left(\overline{\tau}^*/\overline{\tau}_o^*\right)^p\right\}^q\right] \tag{11}$$

where ν_o is the fundamental vibration frequency of the dislocation, $p=1$ and $q=2$ are material constants defining the shape of the short-range obstacle, k_B is the Boltzmann's constant, U_o is the referential activation energy at zero absolute temperature, $\overline{\tau}^*$ is the undamaged thermal stress from Eq. (4), which is a function of strain $\overline{p}$, strain rate $\dot{\overline{p}}$, and temperature T,

$$\overline{\tau}^* = [\overline{Y}_{yp} + \overline{\widehat{R}}][1+(\eta^{vp}\dot{\overline{p}})^{1/m_1}][1-\left(T/T_m\right)^n] \tag{12}$$

and $\overline{\tau}_o^*$ is the referential thermal stress for the intact material at which dislocations can overcome the obstacles without the assistance of thermal activation. Furthermore, ℓ has the following expression [7]:

$$\ell = \frac{d\,D}{D + d\left[1-\exp(-a_1\overline{p})\right]} \tag{13}$$

where d is the mean grain size or mean particle (inclusion) size, D is the mean inter-particle spacing in particle reinforced composites or other characteristic size, p is the effective plastic strain, and a_1 is the strain-hardening rate (see Eq.$(6)_2$). This equation shows that ℓ decreases with the effective plastic strain, increases with the grain size or inclusion size, decreases with the ratio of D/d, and decreases with the strain-hardening rate. It also shows that ℓ decreases from an initial value $\ell = d$ at yielding to a final value $\ell \to 0$ which corresponds to the classical local plasticity or damage limit at very large values of D, d, or p.

The thermodynamic pressure stress P for a shock compressed solid is given as follows:

$$P = (1-\gamma) c_v T^{ig} \varepsilon\,, \quad T^{ig} = T_r \exp\left[(\eta - \eta_r)/c_v\right]\left[1+\varepsilon\right]^{(\gamma-1)} \exp\left[(\gamma-1)\left(1/(1+\varepsilon)-1\right)\right] \tag{14}$$

which gives the equation of state necessary for high-impact loading. The equation of state accounts for compressibility effects (changes in density) and irreversible thermodynamic processes. $\gamma = c_p/c_v$ is the ratio of the specific heats, where c_p and c_v are the specific heats at constant pressure and constant volume, respectively. ε is the nominal volumetric strain, and T^{ig} is chosen to have the form of ideal gas temperature with T_r is the room temperature, η is the entropy, and η_r is the reference entropy. The increase in temperature is calculated using the following heat equation:

$$\rho_o c_p \dot{T} = \Upsilon \boldsymbol{\tau}' : \left(\boldsymbol{d}^{vp} + \boldsymbol{d}^{vd}\right) - J^e P(\boldsymbol{d}^e : \mathbf{1}) - T\boldsymbol{\beta} : \boldsymbol{d}^e \tag{15}$$

where ρ_o is the reference density and Υ is the heat fraction.

In this development we base the failure criterion on the nonlocal evolution of the accumulated micro-damage internal state variable, $\widehat{\boldsymbol{\phi}}$, and the equation of state for the thermodynamic pressure. It implies that for

$$\left\|\widehat{\boldsymbol{\phi}}\right\| = \sqrt{\widehat{\phi}_{ij}\widehat{\phi}_{ij}} \geq \left\|\boldsymbol{\phi}\right\|_c \quad \text{and/or} \quad P \geq P_{cutoff} \tag{16}$$

the material loses its carrying capacity, where $\|\boldsymbol{\phi}\|_c$ is the critical damage when catastrophic failure in the material takes place and P_{cutoff} is the pressure cutoff value when tensile failure or compressive failure occurs.

The proposed model is implemented in the well-known commercial finite element program ABAQUS/Explicit [9] via the user material subroutine VUMAT. Now we conduct a numerical simulation of the experimental tests presented in [8] for a blunt projectile made of hardened Arne tool steel impacting a 12mm thick circular plate made of Weldox 460 E steel. The circular target plate of 500 mm diameter is examined here for different projectile velocities. For simplicity, the projectile is modeled as a bilinear elastic-plastic strain rate-independent von Mises material with isotropic hardening. The nominal length and diameter of the hardened projectile are 80 mm and 20 mm, respectively. The target plate is fully clamped at the edge boundary, while the projectile is given an initial velocity for all simulations. The experimental results in [8] indicated the problem involving shear localization and plugging for blunt projectiles. The numerical solution using the present model is mesh size independent and converges monotonically towards a limit solution when the number of elements over the target thickness becomes sufficiently large. The proposed model can predict the shear localization behavior with no finite element mesh dependency.

The plot of the initial configuration of one of the FE analysis is shown in Fig. 1. Due to symmetry and in order to reduce the simulation time, an axisymmetric problem is solved, where a four-node 2D axisymmetric element with one integration point and a stiffness based on hourglass control is used, and the mesh is somewhat coarsened towards the boundary.

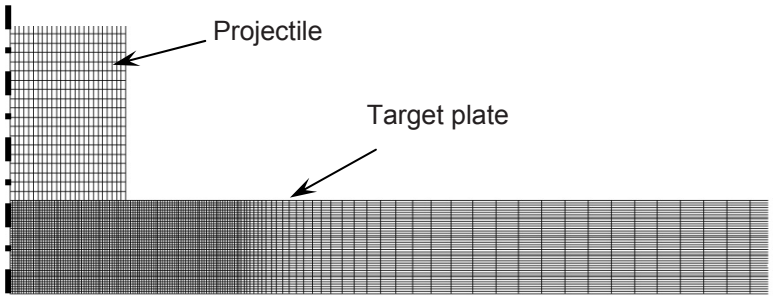

Fig. 1. Finite element mesh plot of the axisymmetric initial configuration just before impact.

Two- and three-dimensional simulations are presented in Figs. 2 and 3. This is done in order to make sure that both types of simulations yield the same results and no dependence on the type of analysis is encountered. Numerical plots showing perforation of the target plate by a blunt projectile at impact velocity close to the ballistic limit of 200m/s are shown in Figs. 2 and 3. The contours of accumulated viscoinelastic strain are plotted on the deformed mesh. It can be seen that limited inelastic deformation occurs outside the localized shear zone. These plots clearly demonstrate that the numerical model qualitatively captures the overall physical behavior of the target during penetration and perforation as compared to the experimental results in Fig. 1. Moreover, the 2-D and 3-D simulations agree very well. Notice also that in these plots, only a part of the complete target plate is shown. High-speed camera images showing perforation of the target plate at impact velocities close to the ballistic limit are shown in Fig. 4, where the numerical simulations are in very well agreement with the simulations.

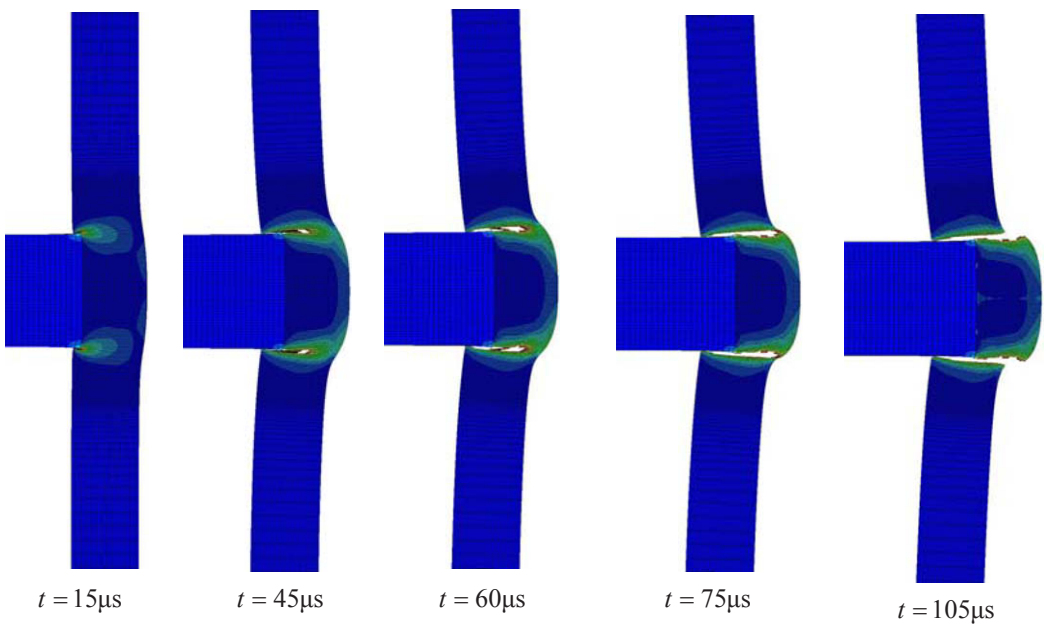

Fig. 2. Two-dimensional numerical simulation of perforation of the target plate by a blunt projectile of initial impact velocity of 200 m/s plotted as contours of accumulated viscoinelastic strain at different times.

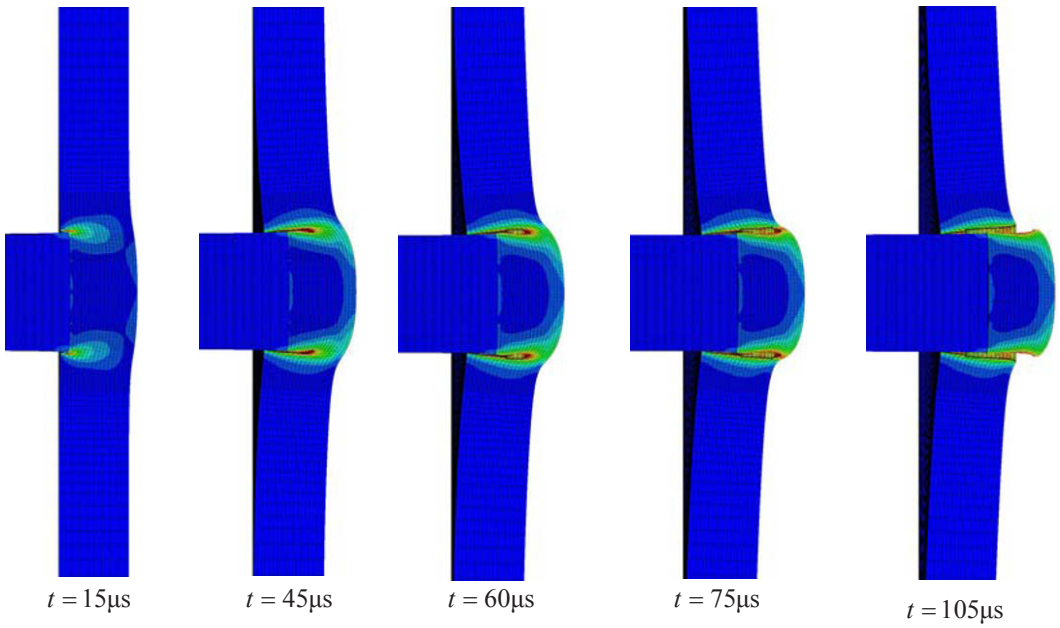

Fig. 3. Three-dimensional numerical simulation of perforation of the target plate by a blunt projectile of initial impact velocity of 200 m/s plotted as contours of accumulated viscoinelastic strain at different times.

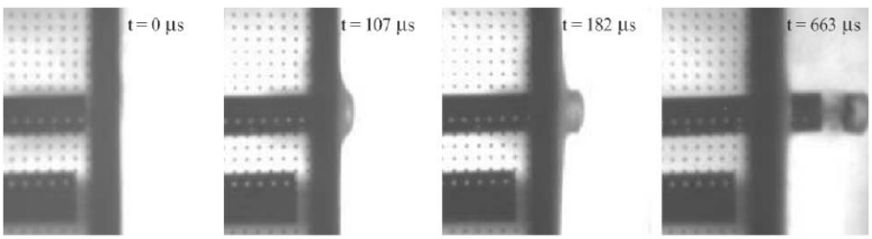

Fig. 4. High-speed camera images showing perforation of the target plate at impact velocities close to the ballistic limits with a blunt projectile; after [8].

Figs. 5(a) and 5(b) shows the impact versus the predicted residual velocity curves for various number of elements through the plate thickness when compared to the experimental data in [8]. Fig. 5(a) shows the current model predictions when assuming a zero length scale $\ell = 0$ (i.e. local damage), while Fig. 5(b) shows the predictions with the nonlocal damage model. It is very clear that mesh sensitivity is most distinct close to the ballistic limit such that the predicted ballistic limit velocity (i.e. at zero residual velocity) when assuming $\ell = 0$ is mesh sensitive. At higher impact velocities, the results are far less affected by the mesh size. However, this mesh sensitivity is alleviated to a great extent when using $\ell \neq 0$ (i.e. nonlocal damage). Also, it is seen from Fig. 5(a) that the ballistic limit velocity decreases as the number of elements through the thickness increases. Therefore, when conducting the ballistic failure simulations using a local damage model, one does not know which mesh density will yield meaningful values for the ballistic limit velocity, which may mislead the design of ballistic protective systems. The proposed nonlocal damage model successfully predicts meaningful values for the ballistic limit; of course, when mesh of sufficient density is used. Also, the nonlocal theory can be used in reducing the computational time by using coarser meshes.

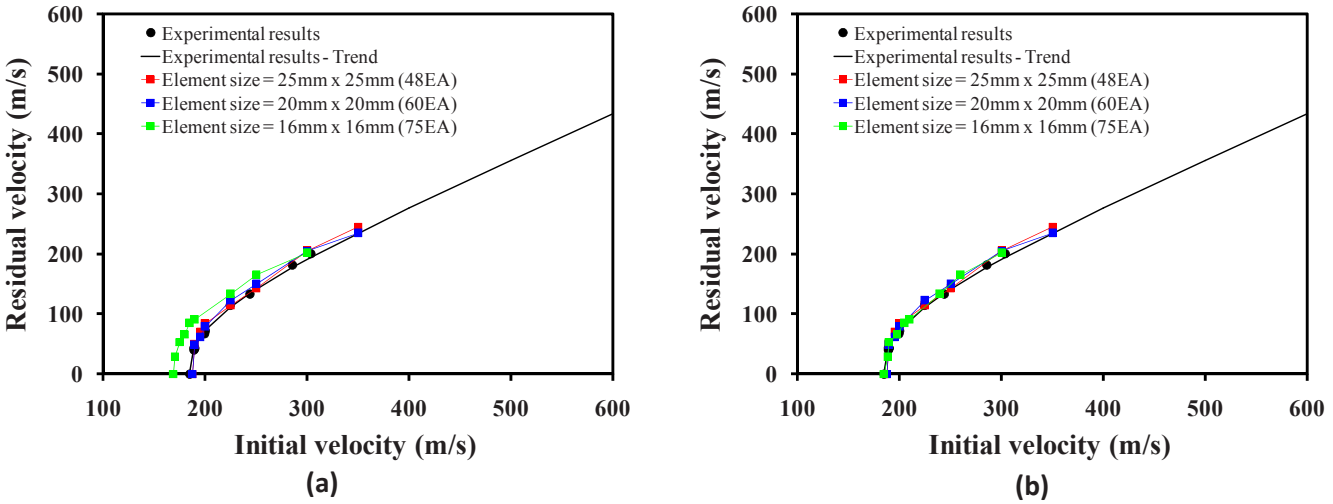

Figure 5. Mesh sensitivity study of the blunt residual velocity versus its initial impact velocity impacting a 12mm thick target when using (a) local damage ($\ell = 0$) and (b) nonlocal damage ($\ell = 7.3\mu m$). Experimental data are after [8].

CONCLUSIONS

A coupled thermo-hypoelasto-viscoplastic and nonlocal gradient-dependent thermo-viscodamage continuum model is utilized in this paper for simulating the ballistic behavior of heterogeneous materials with length scale effects. It is concluded in this paper that an explicit material length scale parameter should be incorporated into the local theories of viscoplasticity and viscodamage in order to predict meaningful values for the ballistic limit velocities independent of the finite element mesh density. Although the presented constitutive equations incorporate length scale parameters implicitly through the viscosity, they are insufficient in predicting mesh objective results of the ballistic behavior of high-strength steel targets impacted by blunt projectiles in which shear plugging due to plastic and damage localization is the dominant mode of failure. This mesh sensitivity is more significant at impact velocities close to the ballistic limit velocity and increases as the target thickness increases. This is attributed to the larger plastic and damage localization as the target thickness increases. Hence, in case of absence of experimental data to check the ballistic results from a specific mesh density, one cannot know if the local model underestimates (conservative) or overestimates (unconservative) the value of the ballistic limit velocity. However, an explicit length scale parameter through the nonlocal damage theory sufficiently alleviates the mesh sensitivity of the ballistic limit velocity allowing one to precisely determine the ballistic limit velocities and describe the overall physical ballistic behavior of targets using numerical simulations. Moreover, it can be concluded that the ballistic limit prediction from the nonlocal theory is a slightly conservative one since it takes into consideration the current damage at a specific point as well as the effect of the surrounding damaged region at that point. Therefore, this desirable feature provided by the nonlocal theory does lead to an improvement in the modeling and numerical simulation of high velocity impact related problems such that numerical simulations could be used in the design process of protective systems against high speed impacts and in providing physical understanding of the ballistic and penetration problem.

ACKNOWLEDGMENT

The work reported in this paper is supported by a grant from the U.S. Army Research Office, and by the Air Force Institute of Technology. These supports are gratefully acknowledged

REFERENCES

[1] Abu Al-Rub, R.K., Voyiadjis, G.Z. “A Finite Strain Plastic-Damage Model for High Velocity Impacts using Combined Viscosity and Gradient Localization Limiters,: Part I-Theoretical Formulation,” International Journal of Damage Mechanics, 15(4), 293-334, 2006.

[2] Voyiadjis, G.Z., Abu Al-Rub, R.K. “A Finite Strain Plastic-Damage Model for High Velocity Impacts using Combined Viscosity and Gradient Localization Limiters, Part II: Numerical Aspects and Simulations,” International Journal of Damage Mechanics, 15(4), 335–373, 2006.
[3] Voyiadjis, G.Z., Abu Al-Rub, R.K., and Palazotto, A.N. “Constitutive Modeling and Simulation of Perforation of Steel Plates by Blunt Projectile,” AIAA Journal, 46(2), 304-316, 2008.
[4] Abu Al-Rub, R.K., Kim, S.-M. “Predicting Mesh-Independent Ballistic Limits for Heterogeneous Targets by a Nonlocal Damage Computational Framework,” Composites: Part B, 40(6), 495-510, 2009.
[5] Abu Al-Rub, R.K. and Voyiadjis, G.Z. “Analytical and Experimental Determination of the Material Intrinsic Length Scale of Strain Gradient Plasticity Theory from Micro- and Nano-Indentation Experiments,” International Journal of Plasticity, 20(6), 1139-1182, 2004.
[6] Abu Al-Rub, R.K., and Voyiadjis, G.Z. “Determination of the Material Intrinsic Length Scale of Gradient Plasticity Theory,” International Journal of Multiscale Computational Engineering, 2, 377-400, 2004.
[7] Voyiadjis, G.Z., Abu Al-Rub, R.K. “Gradient Plasticity Theory with a Variable Length Scale Parameter,” International Journal of Solids and Structures, 42, 3998-4029, 2005.
[8] Børvik, T., Langseth, M., Hopperstad, O.S., Malo, K.A. "Effect of Target Thickness in Blunt Projectile Penetration of Weldox 460E Steel Plates." Int. J. Impact Eng., 28, 413-464, 2003.
[9] ABAQUS. User Manual, Version 6.5, Hibbit, Karlsson and Sorensen, Inc, 2005.